Electroproduction of Kaons on Light Nuclei

B. Zeidman[c], D. Abbott[b], A. Ahmidouch[dfe], P. Ambrozewicz[g], C.S. Armstrong[bh], J. Arrington[ci], R. Asaturyan[j], K. Assamagan[f], S. Avery[f], K. Bailey[c], O.K. Baker[f], S. Beedoe[d], H. Bitao[f], H. Breuer[k], D.S. Brown[k], R. Carlini[b], J. Cha[f], N. Chant[k], E. Christy[f], A. Cochran[f], L. Cole[f], G. Collins[k], C. Cothran[l], J. Crowder[m], W.J. Cummings[c], S. Danagoulian[db], F. Dohrmann[cn], F. Duncan[k], J. Dunne[b], D. Dutta[o], T. Eden[f], M. Elaasar[p], R. Ent[b], L. Ewell[k], H. Fenker[b], H.T. Fortune[q], Y. Fujii[r], L. Gan[f], H. Gao[c], K. Garrow[b], D.F. Geesaman[c], P. Gueye[f], K. Gustafsson[k], K. Hafidi[c], J.O. Hansen[c], W. Hinton[f], H.E. Jackson[c], H. Juengst[s], C. Keppel[f], A. Klein[t], D. Koltenuk[q], Y. Liang[u], J.H. Liu[s], A. Lung[b], D. Mack[b], R. Madey[fe], P. Markowitz[ab], C.J. Martoff[g], D. Meekins[b], J. Mitchell[b], T. Miyoshi[r], H. Mkrtchyan[j], R. Mohring[k], S.K. Mtingwa[d], B. Mueller[c], T.G. O'Neill[c], G. Niculescu[fv], I. Niculescu[fw], D. Potterveld[c], J.W. Price[x], B.A. Raue[ab], P.E. Reimer[c], J. Reinhold[abc], J. Roche[h], P. Roos[k], M. Sarsour[y], Y. Sato[r], G. Savage[f], R. Sawafta[d], J.P. Schiffer[c], R.E. Segel[o], A. Semenov[e], S. Stepanyan[j], V. Tadevosian[j], S. Tajima[z], L. Tang[f], B. Terburg[+], A. Uzzle[f], S. Wood[b], H. Yamaguchi[r], C. Yan$_1$[b], C. Yan$_2$[e], L. Yuan[f], M. Zeier[l], and B. Zihlmann[l]

[a]Florida International University, [b]Thomas Jefferson National Accelerator Laboratory, [c]Argonne National Laboratory, [d]NC A&T State University, [e]Kent State University, [f]Hampton University, [g]Temple University, [h]College of William and Mary, [i]California Institute of Technology, [j]Yerevan Physics Institute, [k]University of Maryland, [l]University of Virginia, [m]Juniata College, [n]Forschungszentrum Rossendorf, [o]Northwestern University, [p]Southern University at New Orleans, [q]University of Pennsylvania, [r]Tohoku University, [s]University of Minnesota, [t]Old Dominion University, [u]American University, [v]Ohio University, [w]The George Washington University, [x]Rensselaer Polytechnic Institute, [y]University of Houston, [z]Duke University, [+]University of Illinois

The A(e,e'K$^+$)YX reaction on H, D, ^{3}He, and ^{4}He was investigated in Hall C at CEBAF. Data were obtained for $Q^2 \approx 0.35$ and 0.5 GeV^2 at 3.245 GeV. The missing mass spectra for both H and D are fitted with Monte-Carlo simulations incorporating peaks corresponding to Λ production on the proton and Σ production on both the proton and neutron. For D, the cross section ratio $\Sigma^0/\Sigma^- \approx 2$, and excess yield close to the thresholds for Λ and Σ production can be attributed to final-state interactions that are compared to the data. The analysis of the data for the He targets is in a more preliminary state with broader quasi-free peaks resulting from the higher Fermi momenta. Evidence for bound Λ-hypernuclear states is seen and other structure may be present.

1. INTRODUCTION

Although hypernuclear interactions have been investigated for many decades, primarily via the use of hadronic probes [1], there is a paucity of data for the electroproduction of

DISCLAIMER

DISCLAIMER

Portions of this document may be illegible in electronic image products. Images are produced from the best available original document.

Kaons that is a result of technical difficulties. The availablility of high-intensity CW electron beams at Jefferson Lab now makes detailed measurements of Kaon electroproduction on light nuclei feasible. The basic equation describing electroproduction of hadrons is:

$$\frac{d\sigma}{d\Omega_{CM}} = \sigma_T + \epsilon\sigma_L + \epsilon\sigma_{TT}\sin^2\Theta\cos(2\phi) + \sqrt{\frac{\epsilon(\epsilon+1)}{2}}\sigma_{LT}\sin\Theta\cos\phi \quad (1)$$

where ϵ is the photon polarization and the other the kinematic variables are defined in Fig. 1. In experiment E91-16, (e,e'K^+) reactions on H and D, and, more recently, ^{3}He and ^{4}He targets have been measured at an incident electron energy of 3.245 GeV in Hall C at CEBAF. Angular distributions of K^+ were obtained at forward angles w.r.t. the virtual photon for $Q^2 \approx 0.35$ and 0.5 GeV^2. While the results for H and D are discussed below, the analysis of the helium data is in its early stages, so that only missing mass distributions and preliminary conclusions for ^{3,4}He(e,e'K^+) are presented.

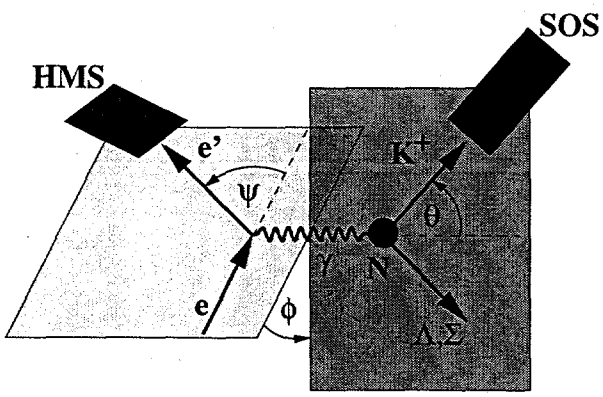

Figure 1. Conceptual description of the H(e, e'K^+)Y reaction. For complex targets, Y is accompanied by nucleons, generally unbound. In E91-16, Θ_k ranges from $0 - -15^o_{\rm lab}$

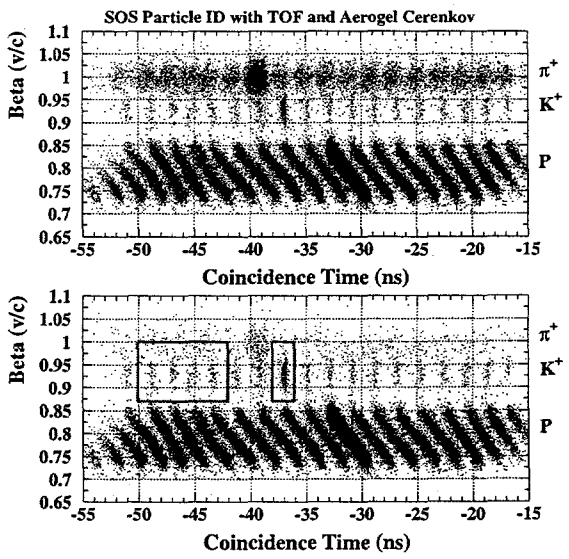

Figure 2. Particle Identification. The top is raw data; below, the threshold for the Aerogel $\hat{C}$ has been reduced offline. Beta $\approx$ distance between hodoscopes/TOF/c.

2. EXPERIMENT

The study of the A(e,e'K^+)YX reaction utilized the HMS and SOS spectrometers to detect the emergent electrons and Kaons, respectively, as in Fig. 1. The detector *system in* each of the spectrometers is similar: a separated pair of multi-plane drift chambers; a pair of X-Y scintillator hodoscopes $\sim$ 1.5 m apart; Cerenkov counters; and a shower counter. A

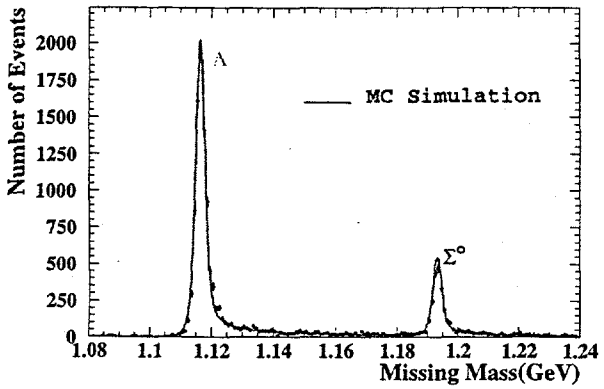

Figure 3. Missing mass spectrum for Hydrogen. The curve is a Monte-Carlo simulation normalized to the data.

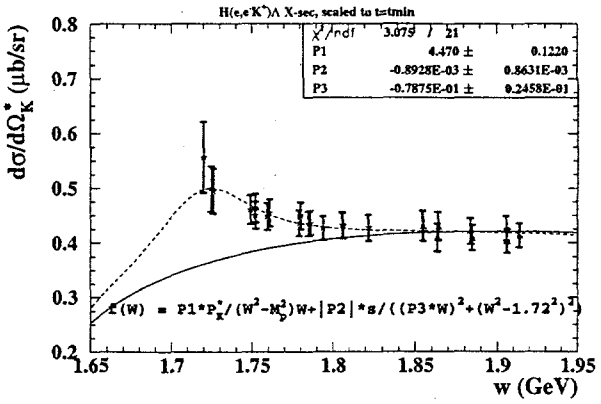

Figure 4. W dependence of the $H(e,e'K^+)\Lambda$ cross section scaled to t_{min}. The dashed curve includes a 'resonance' at ~1.72 GeV in addition to phase space (solid curve).

brief description of the experimental procedure has been published previously [2]. Kaon identification is critically dependent upon measurement of the time difference between the hodoscopes (TOF) and the coincidence time between the HMS and SOS, as illustrated in Fig. 2; the structure in coincidence time being due to the RF strucure of the beam. The locations of true hadron-electron coincidences are darker. As is seen, most of the pions can be eliminated with the Aerogel while random background is eliminated by subtracting properly weighted accidentals. Inasmuch as the acceptance of each spectrometer covers a broad range angles and momentum, the values of the kinematic variables are reconstructed for each event.

3. RESULTS AND DISCUSSION

For e-K coincidences, the mass of the residual system, i.e. the missing mass, is determined from the reconstructed events. The missing mass spectrum for H, after background subtraction, is shown in Fig. 3. The two prominent peaks correspond to Λ and Σ^0 production together with a Monte-Carlo simulation that models spectrometer acceptances and includes radiative effects. From these analyses, with appropriate binning, it is possible to determine [3] various kinematic dependences of the $H(e,e'K^+)\Lambda$ cross section, e.g. the W-dependence seen in Fig.4, as well as t- and Q-dependences. Of particular interest is the Φ-dependence of the cross section along the direction of the virtual photon, Fig. 5, one of the first measurements of the interference terms in Kaon electroproduction Fig. 6 is a missing mass distribution for $D(e,e'K^+)YN$ with background from the target cell walls and accidental coincidences subtracted. The two prominent distributions correspond to Λ production off the proton and the unresolved Σ^0 and Σ^- production off the proton and the neutron, respectively, with widths reflecting the initial momentum distribution of the nucleons in the deuteron. The Monte-Carlo simulations for Kaon production on deuterium treat the reaction as purely quasifree production on a nucleon with an initial

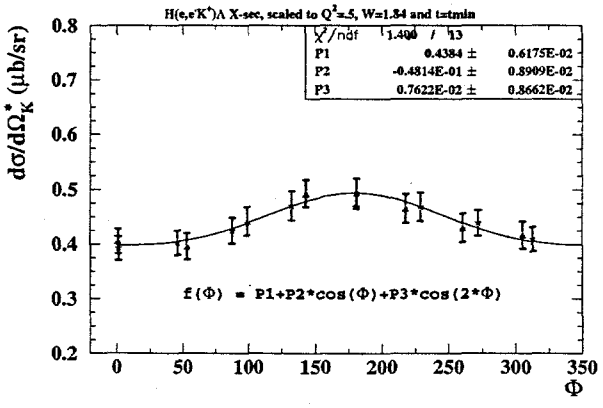

Figure 5. Φ-dependence of the Λ Cross section, P2 and P3 correspond to the L-T and T-T interference terms, respectively, in eq. (1) P2 is $\sim 10\%$ of the the average, P1, and P3 is not statistically significant.

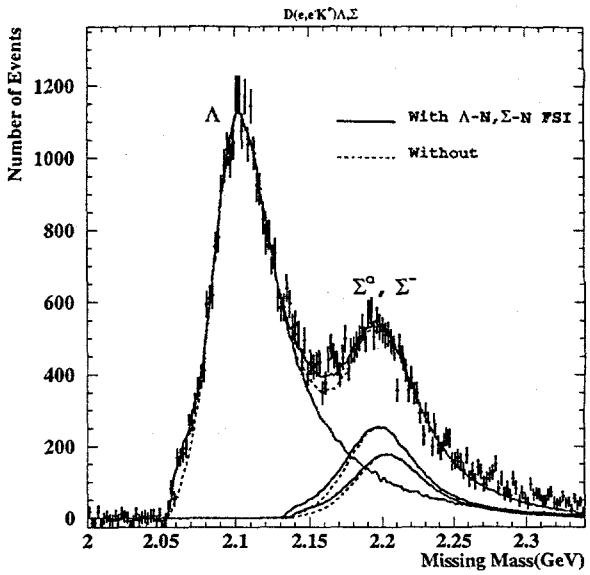

Figure 6. Missing mass distribution for $D(e,e'K^+)YN$ at $\Theta = 1.5^o$ and $Q^2 = 0.38\,GeV^2$. The solid (dashed) lines show simulations with (without) the inclusion of FSI for Λ, Σ^0, Σ^-, and their sum. Note that $\Sigma^0 \sim 2\Sigma^-$.

momentum distribution determined from wave functions calculated with the Bonn potential [4]; the Λ/Σ^0 ratio being obtained from the H data. After subtraction of the 'proton' contribution, the 'neutron' contribution (Σ^-) is obtained. The results of these quasifree simulations for the individual contributions from the Λ, Σ^0, and the Σ^- channels together with their sum are shown in Fig. 6. See ref. [3] for details. While agreeing well with the overall shape of the observed distribution, slightly above the thresholds for both Λn and ΣN this purely quasifree simulation underpredicts the observed yield. In the regions of low relative momenta in the residual hyperon-nucleon system, their mutual interaction, the Final-State Interaction (FSI), leads to a distortion of their respective wave functions, thereby increasing the observed yield.

Following a description by Li and Wright [5] three Λ-nucleon potentials (Verma, Jülich A & B) were parameterized with double-gaussian potentials. In ref. [5], the parameters were adjusted to reproduce the phase shifts of these potentials and the corresponding scattering lengths, and effective ranges. From these parameterizations, the s-wave and p-wave phase shifts were calculated as functions of the Λ-neutron relative momenta and the associated phase-space enhancement determined [3]. A similar approach is employed for the Σ-nucleon final states. The results obtained with the Jülich A potential are shown as the solid lines in Fig. 6 where the observed enhancements above the Λ and ΣN thresholds are both consistent with the FSI model. The ratio of the total FSI contribution to that of the pure quasi-free peak for the Σs is, however, $\sim$7x larger than for the Λ, a value

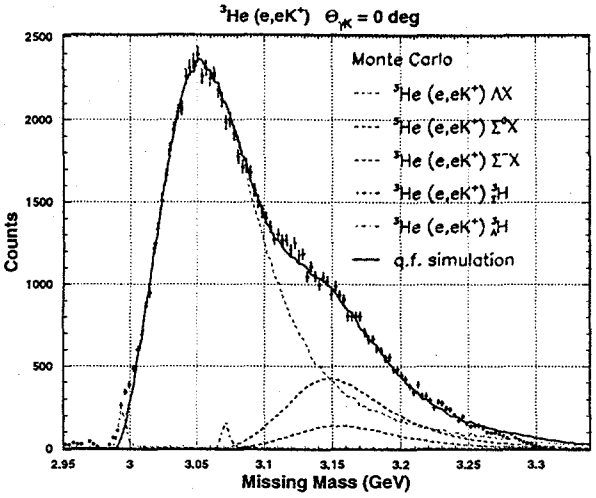

Figure 7. Missing mass distribution for ^{3}He(e, e'K$^+$. The dashed curves represent Monte-Carlo simulations for contributions for the various channels shown; the narrow peaks are locations for possible bound states.

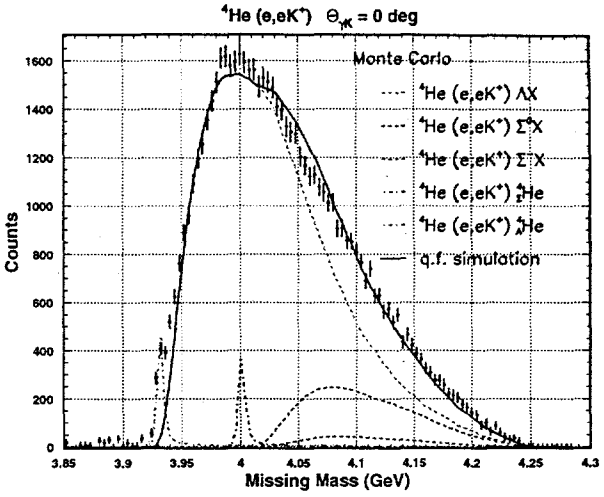

Figure 8. Missing mass distribution for ^{4}He(e, e'K$^+$. The dashed curves represent Monte-Carlo simulations for contributions for the various channels shown. The solid lines are the sums of the quasi-free terms only.

consistent with the possibility of one-pion interactions in the Σ-N channel. The remaining structure still leaves room for more speculative explanations like interference cusps or even bound systems. If it is assumed that Σ production on the proton and neutron is the same except for their isospin, then the ratio of production cross sections should simply reflect isospin coupling coefficients. The observed Σ^0/Σ^- ratio implies I=3/2 in the propagator, rather than I=1/2, a value consistent with the 'resonance' seen in Λ production on the proton.

Preliminary analysis of the He data is shown in Figs. 7 and 8, where because of the increased Fermi motion in the targets, the separation between the two distributions associated with quasifree Λ and Σ production is much less pronounced than in D. At the Λ-threshold, both figures show an enhancement relative to a purely quasifree reaction mechanism. Bound hypernuclear states and, possibly, final-state interactions should be responsible for this excess yield. In this preliminary stage of the Monte-Carlo simulations, neither bound states nor final-state interactions have not been included; the expected positions of Λ- and Σ- bound states are shown. While the ^{3}He data is only suggestive of a bound state, the ^{4}He distribution shows clear evidence for the Λ-bound state at low missing mass. Although the resolution does not yet allow separation of the ground and first excited states of $^4_\Lambda$H, the continuing analysis of the data is expected to clearly identify the peak.

4. SUMMARY

Studies of the (e,e'K$^+$) reaction on light nuclei have provided substantial new information for targets of H and D. Various kinematic dependences for Λ and Σ production

on light nuclei have been determined and the Σ^- cross section on the neutron measured. Final-state interactions in the YN system have been observed and models shown to exhibit sensitivity to different potential parameterizations. Ratios of cross sections in D(e,e'K^+)ΣN reactions imply an I=3/2 propagator near threshold, consistent with a 'resonance' near threshold in Λ production. Data for ^{3,4}He(e,e'K^+) are still in the early stages of analysis, evidence for bound states is observed.

5. ACKNOWLEDGEMENTS

This work was supported in part by the U.S. Department of Energy and the National Science Foundation. The author acknowledges support from Argonne National Laboratory and the U.S. Dept. of Energy under contract No. W-31-109-Eng-38 and is particularly grateful for assistance provided by F. Dohrmann, currently at ANL as a Feodor Lynen Fellow of the A. v. Humboldt Foundation.

REFERENCES

1. Proceedings of the International Conference on Hypernuclear and Strange Particle Physics, ed. by D. J. Millener and R. E. Chrien, Nucl. Phys. A639 (1998).
2. D. Abbott et al., Nucl. Phys. A639 (1998) 197c.
3. J. Cha, Ph.D. thesis, Hampton University, 2000.
4. T.S. Lee, private communication.
5. X. Li and L.E. Wright, J. Phys. G 17 (1991) 1127.